

Study of the $^{13}_{\Lambda}$ C hypernucleus by the $^{13}\text{C}(K^-, \pi^-\gamma)$ reaction

H. Kohri, S. Ajimura, H. Hayakawa, T. Kishimoto, K. Matsuoka, S. Minami, Y. S. Miyake, T. Mori, K. Morikubo, E. Saji, A. Sakaguchi, Y. Shimizu, and M. Sumihama

Department of Physics, Osaka University, Toyonaka, Osaka, 560-0043, Japan

R. E. Chrien, M. May, P. Pile, A. Rusek, and R. Sutter

Brookhaven National Laboratory, Upton, New York 11973, USA

P. M. Eugenio, G. Franklin, P. Khaustov, K. Paschke, B. Quinn, and R. A. Schumacher

Department of Physics, Carnegie Mellon University, Pittsburgh, PA 15213, USA

J. Franz

Department of Physics, University of Freiburg, D79104 Freiburg, Germany

T. Fukuda, H. Noumi, and H. Outa

High Energy Accelerator Research Organization (KEK), Tsukuba, Ibaragi, 305-0801, Japan

L. Gan, L. Tang, and L. Yuan

Department of Physics, Hampton University, Hampton, VA 23668, USA

J. Nakano, T. Tamagawa, and K. Tanida

Department of Physics, University of Tokyo, Tokyo 113-0033, Japan

R. Sawafta

Department of Physics, North Carolina A T State University, Greensboro, NC 27411, USA

H. Tamura

Department of Physics, Tohoku University, Sendai 980-8578, Japan

H. Akikawa

Department of Physics, Kyoto University, Kyoto 606-8502, Japan

(May 21, 2019)

Abstract

The ${}^3_\Lambda\text{C}$ hypernucleus was studied by measuring γ rays in coincidence with the ${}^{13}\text{C}(K^-, \pi^-)$ reaction. γ rays from the $1/2^-$ and $3/2^-$ states, which are the partners of the spin-orbit doublet states with a predominant configuration of $[{}^{12}\text{C}_{g.s.}(0^+) \otimes p_\Lambda]$, to the ground state were measured. The splitting of the states was found to be $\Delta E(1/2^- - 3/2^-) = +152 \pm 54(\text{stat}) \pm 36(\text{syst})$ keV. This value is 20~30 times smaller than that of single particle states in nuclei around this mass region. The $j_\Lambda = \ell_\Lambda - 1/2$ ($(p_{1/2})_\Lambda$) state appeared higher in energy, as in normal nuclei. The value gives new insight into the YN interaction. The excitation energies of the $1/2^-$ and $3/2^-$ states were obtained as $10.982 \pm 0.031(\text{stat}) \pm 0.056(\text{syst})$ MeV and $10.830 \pm 0.031(\text{stat}) \pm 0.056(\text{syst})$ MeV, respectively. We also observed γ rays from the $3/2^+$ state, which has a $[{}^{12}\text{C}(2^+) \otimes s_\Lambda]$ configuration, to the ground state in ${}^3_\Lambda\text{C}$. The excitation energy of the $3/2^+$ state was obtained as $4.880 \pm 0.010(\text{stat}) \pm 0.017(\text{syst})$ MeV. Nuclear γ rays with energies of 4.438 and 15.100 MeV had similar yields, which suggests that a quasi-free knockout of a Λ particle is dominant in highly excited regions.

PACS numbers: 21.80.+a, 25.80.Nv, 13.75.Ev, 26.60.+c

I. INTRODUCTION

The introduction of the spin-orbit (ℓs) force, which is a short range interaction, resulted in great successes of the nuclear shell model. Before this introduction, the central force described by the harmonic oscillator had been unable to explain magic numbers except for 2, 8, and 20. The ℓs -force clearly explained not only the magic numbers but also many prominent nuclear properties. The ℓs -splitting of single nucleon states is as large as that of the major shell spacing and plays an essential role in nuclear physics.

As for Λ -nucleus interactions in Λ -hypernuclei, the observation of Λ single particle states, first by the (K^- , π^-) reaction [1] and then later by the (π^+ , K^+) reaction [2,3], clarified the gross structure of the interactions. The central force was found to be roughly 2/3 of that of a nucleon. In the naive quark model a Λ particle is composed of u, d, and s quarks and the s (strange) quark is considered to contribute little to the nuclear force. In the one boson exchange (OBE) model it is understood that the absence of the long-range one pion exchange contribution makes the central force smaller. On the other hand, spin-dependent forces are not well known. Especially, the ℓs -force in a Λ -nucleus is considered to be much smaller than that in a nucleon-nucleus, although no experiment has given a conclusive value. Measurement of the Λ -nucleus ℓs -splitting has been one of major objects in the study of hypernuclei for more than two decades.

This paper is a follow-up to our recently-published paper [4] which was confined to the derivation of the ℓs -splitting. In this paper, details of the experiment and analysis are provided and spectroscopic results for the ${}^3_\Lambda C$ hypernucleus are discussed.

A. Experimental studies

The first indication of a small Λ -nucleus ℓs -splitting was given by the study of the ${}^{16}_O(K^-, \pi^-){}^{16}_\Lambda O$ reaction at the CERN Proton Synchrotron (PS) [5] in 1978. They observed peaks with major configurations of $[(p_{1/2})_n^{-1}(p_{1/2})_\Lambda]_{0^+}$ and $[(p_{3/2})_n^{-1}(p_{3/2})_\Lambda]_{0^+}$. The splitting of the two peaks was about 6 MeV which is quite close to 6.18 MeV corresponding to a splitting between the $(p_{1/2})_n^{-1}$ and $(p_{3/2})_n^{-1}$ states in ${}^{15}O$ (core nucleus of ${}^{16}_\Lambda O$). This result suggested that the Λ - ${}^{15}O$ ℓs -force was extremely small. Brückner *et al.* gave an upper limit of 0.3 MeV for the ℓs -splitting. However a detailed theoretical analysis gave 0.8 ± 0.7 MeV for the splitting [6]. Consequently the constraint on the splitting was weakened. Later May *et al.* measured an energy shift of a peak at $E_x \sim 10.4$ MeV between 0° and 15° by the ${}^{13}C(K^-, \pi^-){}^{13}_\Lambda C$ reaction at the AGS of BNL [7]. Predominant configurations of the peak were $[(p_{1/2})_n^{-1}(p_{1/2})_\Lambda]_{1/2^-}$ at 0° and $[(p_{1/2})_n^{-1}(p_{3/2})_\Lambda]_{3/2^-}$ at 15° . They obtained 0.36 ± 0.3 MeV for the splitting of the $1/2^-$ and $3/2^-$ states in ${}^{13}C$. Another study was the observation of γ rays from ${}^9_\Lambda Be$ excited by the ${}^9Be(K^-, \pi^-)$ reaction by using NaI detectors [8]. A peak was observed at 3.079 ± 0.040 MeV in the γ ray spectrum and the peak was considered to be due to γ rays from unresolved $3/2^+$ and $5/2^+$ states, which have a configuration of $[{}^8Be(2^+) \otimes (s_{1/2})_\Lambda]$, to the ground state (GS) in ${}^9_\Lambda Be$. The width of the peak suggested that the splitting was less than 0.1 MeV, although the possibility that γ rays from either state were missing was not completely excluded.

On the other hand, data suggesting larger ℓs -splittings appeared recently. Nagae *et al.* observed a series of peaks considered to be associated with states with a Λ particle in the s ,

p, *d*, and *f*-orbits by the $^{89}\text{Y}(\pi^+, K^+)_{\Lambda}^{89}\text{Y}$ reaction at KEK-PS [9]. The widths of the peaks seemed to be broader for larger ℓ states. Since the ℓs -splitting increases almost linearly with the orbital angular momentum, the peaks could be interpreted as unresolved ℓs -doublets with $V_{\ell s} \sim 6$ MeV by using the Woods-Saxon prescription. This result was further supported by the re-analysis of the emulsion data of $^{16}\Lambda\text{O}$ collected by the European K^- collaboration [10]. Dalitz *et al.* assigned configurations of $[(p_{1/2})_n^{-1}(p_{1/2})_{\Lambda}]_{0+}$ and $[(p_{1/2})_n^{-1}(p_{3/2})_{\Lambda}]_{2+}$ to two peaks which were separated by 1.56 ± 0.12 MeV. They derived splitting consistent with the $^{89}\Lambda\text{Y}$ data.

B. Theoretical studies

Interactions between baryons have been studied by the meson exchange theory combined with phenomenology. The OBE model of the nucleon-nucleon (NN) interaction was extended to the hyperon-nucleon (YN) interaction with the help of flavor SU(3) symmetry [11]. Effective one-body hyperon-nucleus interactions were constructed based on the OBE models [12,13]. They well reproduce the central part of the Λ -nucleus interaction and predict a weak Λ -nucleus ℓs -force. For example, the ℓs -splitting of Λ single particle states in $^{13}\Lambda\text{C}$ was calculated to be 0.56 MeV, $E_x = 10.56$ MeV for $(p_{1/2})_{\Lambda}$ and $E_x = 10.00$ MeV for $(p_{3/2})_{\Lambda}$ [14]. The ℓs -splitting was $0.1 \sim 0.2$ of that of single nucleon states (3~5 MeV).

There has been another attempt to study the short-range part of the NN interaction from a standpoint that baryons are made of quarks and the short-range part of baryon-baryon interactions should be understood by quark and gluon exchanges. Morimatsu *et al.* studied the ℓs -force between baryons within the framework of a nonrelativistic quark-cluster model [15]. Since this model had a strong anti-symmetric spin-orbit (ALS) force, which was opposed to the symmetric ℓs -force, it gave a very small Λ -nucleus ℓs -splitting. Pirner and Povh also predicted zero splitting for the Λ -nucleus ℓs -splitting [16].

As described above, the quark models tend to predict small Λ -nucleus ℓs -splittings compared with those of the OBE models. A new experiment with a precision of better than 0.1 MeV for the ℓs -splitting has been needed to distinguish the models.

C. The $^{13}\Lambda\text{C}$ hypernucleus

The $1/2^-$ and $3/2^-$ states in $^{13}\Lambda\text{C}$ are ideal states to extract the ℓs -splitting. It is well known that the $1/2^-$ and $3/2^-$ states have predominant configurations of $[^{12}\text{C}_{g.s.}(0^+) \otimes (p_{1/2})_{\Lambda}]$ and $[^{12}\text{C}_{g.s.}(0^+) \otimes (p_{3/2})_{\Lambda}]$, respectively. The two states are the partners of the ℓs -doublet states. By virtue of the 0^+ spin of the ^{12}C core, the energy difference between the states gives the ℓs -splitting of a Λ particle in the *p*-orbit. Recently γ rays from the $1/2^-$ state to the GS were observed at 10.95 MeV by using NaI detectors [17]. This was the first observation of the $p_{\Lambda} \rightarrow s_{\Lambda} \gamma$ ray transition.

II. EXPERIMENT

A. Principles

The ℓs -splitting has been measured mostly by using magnetic spectrometers. The best energy resolution that magnetic spectrometers have achieved in the study of hypernuclei is around 2 MeV (FWHM). Since the ℓs -splitting is predicted to be 0~1 MeV, measurement with a precision of better than 0.1 MeV is necessary. In order to improve the energy resolution, we measured γ rays from the $1/2^-$ and $3/2^-$ states at $E_x \sim 11$ MeV to the GS in $^{13}\Lambda$ C by using NaI detectors. The energy resolution of the NaI detectors was about 0.35 MeV (FWHM) for the detection of 11 MeV γ rays. It was good enough for the measurement of the ℓs -splitting with a precision of better than 0.1 MeV given enough statistics. If the splitting is larger than or close to the energy resolution of the NaI detectors, one should observe two peaks, or a peak clearly broader than the energy resolution, from which one can derive the splitting easily.

Even if the splitting is much less than the energy resolution, the splitting can be derived as follows. The (K^-, π^-) reaction at forward angles is a unique way to selectively excite the $1/2^-$ state in $^{13}\Lambda$ C via the $\Delta\ell=0$ transition. The so-called substitutional transition $((p_{1/2})_n \rightarrow (p_{1/2})_\Lambda)$ is dominant at momentum transfers much smaller than the Fermi momentum. On the other hand the $3/2^-$ state is mainly excited at larger angles (10~20 degrees) of the (K^-, π^-) reaction via the $\Delta\ell=2$ transition. Angular distributions of the $^{13}\text{C}(K^-, \pi^-)^{13}\Lambda$ C reaction for the $1/2^-$ and $3/2^-$ states at 0.9 GeV/c, calculated by Motoba *et al.* with the distorted wave impulse approximation (DWIA) [18], are shown in Fig.1. One can simultaneously excite both states in an experiment and control the ratio of the $1/2^-$ and $3/2^-$ states in an analysis by utilizing the angular distributions. This method tells us not only the splitting but also which state has higher or lower energy.

Based on these considerations we designed an experiment to measure γ rays from the $1/2^-$ and $3/2^-$ states which were excited by the $^{13}\text{C}(K^-, \pi^-)^{13}\Lambda$ C reaction [19].

B. Experimental setup

The experiment (AGS-E929) was carried out by using the D6 beam line [20] of the alternating-gradient synchrotron (AGS) at Brookhaven National Laboratory (BNL). The K^- beam momentum was 0.93 GeV/c, or close to 0.9 GeV/c at the target center after energy loss, in order to maximize the production rate of the $1/2^-$ and $3/2^-$ states in $^{13}\Lambda$ C. The typical K^- beam intensity was about 8×10^4 /spill for 5×10^{12} protons /spill at the primary target. A spill consisted of 1.4 seconds of continuous beam every 4 seconds. The typical ratio of $(\pi^- \mu^- e^-)/K^-$ was 0.3. The intensity and purity of the K^- beam provided by the D6 beam line greatly exceeded those available elsewhere.

The momentum of incoming beam particles was measured using information from a scintillator hodoscope located at the exit of the first mass slit in the beam line and from two drift chambers [20]. Incoming K^- particles were identified electrically using a plastic scintillator (BS), an aerogel Čerenkov counter, and a quartz Čerenkov counter (BQC). The aerogel Čerenkov counter, which had an aerogel block with the refractive index of 1.03, was installed downstream of the two drift chambers. The BQC, which was a total reflection type Čerenkov counter, was installed in front of the target. The detection efficiency for the incoming K^- particles was greater than 99 %. The time-of-flight between a scintillator

hodoscope in the beam line and a timing counter at the exit of the beam line was also used to identify the incoming K^- beam particles in the off-line analysis. The K^- beam was focused on the target in the vertical direction by the last beam line quadrupole magnet. The size of the K^- beam was 5.0 cm (FWHM) in the horizontal direction and 1.1 cm (FWHM) in the vertical direction at the target.

The detector configuration around the target is shown in Fig.2. The target had four cells with inner dimensions of 6 cm wide, 1.5 cm high, and 3 cm thick and containing ^{13}C benzene enriched to 99 %. Each target cell was made of quartz with a wall thickness of 1 mm. Accordingly, the target had some contamination of O and Si nuclei. In the ^{13}C benzene, laser dyes were added to make the target scintillate. It is known that the (K^-, π^-) reaction is strongly contaminated by K^- in-flight decays. The production of $^{13}\Lambda$ hypernuclei was identified by the light output of the scintillating target, and it was possible to discriminate against K^- decay events. Without using this method, the production of $^{13}\Lambda$ hypernuclei could not be clearly observed at certain angles where the kinematics of the K^- decays was the same as that of the $^{13}\text{C}(K^-, \pi^-)^{13}\text{C}$ reaction. The tagging efficiency for the ^{13}C weak decay was greater than 80 % by selecting events with higher light output. Four plastic scintillators (DEC) were installed above and below the target to increase the tagging efficiency for the weak decay by detecting decay particles from near the surface of the scintillating target. The size of each scintillator was 15 cm \times 24 cm \times 1.5 cm. Event selection using the DEC and the scintillating target is described in Sec.III A and details are given in Ref. [21,22].

72 NaI detectors (6 \times 6 above and 6 \times 6 below the target) were installed at a distance of 10.5 cm from the target center. The segmentation was important to withstand high counting rates and was also quite convenient to correct for γ ray Doppler shift. The size of each NaI crystal was 6.5 cm \times 6.5 cm \times 30 cm. A 2" PM tube (Hamamatsu H1161), which was covered with triple magnetic shield cases, was connected to the crystal through a silicon rubber disk and a light guide. The typical counting rate was 5×10^3 counts/spill. High voltages supplied to the PM tubes were set lower than the usual values for stable operation, and TFA's (timing filter amplifiers) were used. An 11 MeV γ ray is energetic enough to make an electromagnetic shower in a NaI crystal. In most cases one detector, called the central detector, received the main energy deposit and neighboring detectors had smaller energy deposits because only 511 keV annihilation γ rays dominantly escaped from the central detector. For increasing the full energy peak efficiency, the energy deposit of 0.1~1.2 MeV in each of three detectors was added up. Since the energy resolution was mainly determined by that of the central detector, NaI detectors with good energy resolution were installed in the center of the NaI array. Eight plastic scintillators (Charge Veto) were installed on the surface of the NaI array to reject the charged particle background. The size of each scintillator was 42 cm \times 10 cm \times 1 cm. When both a charged particle and a γ ray passed through the same element of the Charge Veto, it rejected not only the charged particle but also the γ ray. Thus, the detection efficiency of the NaI detectors for γ rays was decreased by 10 %. The total detection efficiency of the NaI detectors for 11 MeV γ rays was 4.5 % most of which was determined by the geometry.

π^- particles were identified by using an aerogel Čerenkov counter (FAC) with an aerogel refractive index of 1.035. The energy threshold of the discriminator for the FAC was set higher than the single photon signal in order to suppress the trigger rate. This was necessary since the K^- beam produced a strong contamination due to δ rays in particular at forward

angles. However, the higher threshold decreased the detection efficiency of the FAC to 91 % for π^- particles. Scattered π^- particles were bent vertically and analyzed by the 48D48 spectrometer with five drift chambers [23,24]. The efficiency of track reconstruction was 61 % for the (K^-, π^-) reaction. Scintillator hodoscopes defined the acceptance which was -8° to 8° in the horizontal direction and -16° to 0° in the vertical direction. In Fig.3, the acceptance obtained for the $^{13}\text{C}(K^-, \pi^-)$ reaction is shown. There are no unexpected structures due to the inefficiency of detectors. The large acceptance was essential to excite the doublet states simultaneously, which enabled us to derive the splitting with a small systematic error. Time-of-flight [25] was only used to remove the K^- beam background.

The average live time of the DAQ system was 78 %. The $^{13}\text{C}(K^-, \pi^-)$ data were accumulated by using 1.4×10^{10} K^- beam particles in total.

C. Energy calibration of the NaI detectors

The energy calibration of NaI detectors is particularly important for the precise measurement of γ rays. For the energy calibration in the low energy region, we used γ rays from ^{22}Na sources (0.511, 1.275 MeV). A ^{22}Na source was sandwiched between two small plastic scintillators to provide a light signal for a trigger by its β -decay, and they were attached to a 3/8" PM tube. For the energy calibration in the high energy region near 11 MeV, the $^{58}\text{Ni}(n, \gamma)^{59}\text{Ni}$ reaction was used. When a neutron emitted by a ^{244}Cm - ^{13}C source thermalizes in a moderator and is captured by a ^{58}Ni nucleus, a γ ray (8.999 MeV) from the neutron threshold to the GS in ^{59}Ni is emitted. A typical energy spectrum of a central NaI detector obtained in the energy calibration run using the $^{58}\text{Ni}(n, \gamma)^{59}\text{Ni}$ reaction is shown in Fig.4 where only single hit events, which means that there was no signal in neighboring detectors, were selected to make full energy peaks dominant. A full energy peak at 9.0 MeV is observed separated from the 8.5 MeV peak which consists of a single escape peak and γ rays from the neutron threshold to the state at $E_x=0.465$ MeV in ^{59}Ni . Since the expected energy of the reaction γ rays is close to 11 MeV, the systematic error coming from the uncertainty in the energy extrapolation from 9.0 MeV to 11 MeV is small. The largest peak at 6.1 MeV, which was also used for the energy calibration, originates from γ rays emitted by the $^{13}\text{C}(\alpha, n)^{16}\text{O}^*$ reaction in the ^{244}Cm - ^{13}C source. γ rays with energies of 8.999, 6.129, 1.275, and 0.511 MeV and a pedestal were used for the energy calibration under beam-off conditions, and a fit to the five data points with the same weight was successfully performed with a linear function for each NaI detector.

Under beam-on conditions, the energy calibration of the whole system was monitored by ^{22}Na sources for stability over more than a few days. In addition, LED light fed into all NaI detectors was used to monitor the stability over short time durations. The gain shift during a beam spill was less than one percent in the worst case, which was acceptable for the present measurement.

For γ rays from the Λ bound region of ^{13}C , a Doppler shift correction was performed. A recoil momentum vector of a ^{13}C nucleus was obtained from the momentum and direction of incoming K^- and outgoing π^- particles. The direction of an emitted γ ray was calculated from a reconstructed vertex of the (K^-, π^-) reaction and the position of the NaI crystal which had the maximum energy deposit.

As the final energy calibration, we used γ rays with energies of 4.438 and 15.100 MeV from ^{12}C nuclei excited by the quasi-free (K^-, π^-) reaction. The energy calibration using known γ rays simultaneously measured by the $^{13}\text{C}(K^-, \pi^-)_{\Lambda}^{13}\text{C}$ reaction enabled us to determine γ ray energies with small systematic errors. The excitation energy of a state was obtained from the γ ray energy by correcting for the recoil of $_{\Lambda}^{13}\text{C}$ hypernuclei due to emitting γ rays.

III. RESULTS

A. Event selection

Fig.5(a) shows a 2-dimensional spectrum derived from about 10 % of all data taken at $0^\circ < \theta_\pi < 16^\circ$. It shows the momentum of the outgoing particles versus the lab scattering angle before event selection. The main feature is due to K^- beam particles that fired the FAC by δ rays and were not rejected by the hardware trigger. Other loci correspond to K^- in-flight decays. The upper decay locus is $K^- \rightarrow \mu^- + \bar{\nu}_\mu$ ($K_{\mu 2}$, 63.5 %) and the lower is $K^- \rightarrow \pi^- + \pi^0$ ($K_{\pi 2}$, 21.2 %). Since the (K^-, π^-) reaction is strongly contaminated by the background described above, $^{13}\text{C}(K^-, \pi^-)_{\Lambda}^{13}\text{C}$ events are difficult to be clearly observed without the event selection. The $^{13}\text{C}(K^-, \pi^-)_{\Lambda}^{13}\text{C}$ events are observed as a small bump on the huge background in Fig.5(b) which is an excitation energy spectrum of $_{\Lambda}^{13}\text{C}$. The excitation energy was calibrated by using the K^- decay kinematics.

In the first stage, events with at least one 1~20 MeV γ ray, which amounted to about 7 % of all data, were selected. After the first stage the $K_{\mu 2}$ decay and K^- beam events were suppressed. But the $K_{\pi 2}$ decay still remained, as shown in Fig.5(c and d), because a π^0 particle decays mainly by emitting two γ rays.

In the second stage, event selection by using the DEC and the scintillating target outputs was performed to remove most of the remaining background. Events with an energy deposit above threshold either in the DEC or in the scintillating target were selected. The energy threshold of the DEC was set at 2.6 MeV which was lower than the minimum ionization, and that of the scintillating target was set at 1.2 times higher than the minimum ionization peak. This selection tagged 89 % of $_{\Lambda}^{13}\text{C}$ production events and suppressed the K^- decays by 90 %. In addition, outgoing K^- particles were removed by using time-of-flight. Loose vertex cuts of the (K^-, π^-) reaction for the x and y directions were performed, but that for the z direction was not done because it might have caused low efficiency at forward angles. After the second stage a locus corresponding to $^{13}\text{C}(K^-, \pi^-)_{\Lambda}^{13}\text{C}$ events is clearly observed, and most of the K^- decays disappeared as shown in Fig.5(e). In Fig.5(f) a quasi-free peak is clearly observed, although the spectrometer's energy resolution of about 15 MeV (FWHM) could not resolve excited states. The excitation energy of 0 to 25 MeV was selected to purify γ rays from the Λ bound region (0~11.7 MeV), and the energy region of 30 to 100 MeV was regarded as the quasi-free region to observe γ rays from ^{12}C nuclei.

B. Low energy γ rays

Fig.6 shows γ ray spectra in the low energy region obtained in coincidence with the $^{13}\text{C}(K^-, \pi^-)$ reaction at $0^\circ < \theta_\pi < 16^\circ$, where (a) shows γ rays from the quasi-free region and

(b) shows those from the Λ bound region. The Doppler shift due to the recoil of a ${}_{\Lambda}^{13}\text{C}$ nucleus was corrected for event-by-event only in Fig.6(b).

In Fig.6(a), a peak at around 4.5 MeV, which corresponds to γ rays from the first 2^+ state in ${}^{12}\text{C}$, is the strongest feature. The 2^+ state in ${}^{12}\text{C}$ is considered to be copiously produced by the Λ escape from highly excited states in ${}_{\Lambda}^{13}\text{C}$. It is well understood that neutron pickup reactions, such as the ${}^{13}\text{C}(\text{p}, \text{d})$ reaction [26], strongly excite the 2^+ state. As a result of fitting, the peak position was obtained as $4.467 \pm 0.005(\text{stat})$ MeV which was shifted to higher energy by 29 keV. A rate-dependent gain shift is believed to be the main reason for the apparent energy shift. We used the energy shift for the energy calibration to obtain the correct energy of γ rays from ${}_{\Lambda}^{13}\text{C}$ hypernuclei. The width of the 2^+ peak is $240 \pm 10(\text{stat})$ keV (FWHM) which is reasonable. Other peak structures are thought to be due to γ rays from ${}^{27}\text{Si}$ or ${}^{15}\text{O}$ nuclei produced by the quasi-free process.

In Fig.6(b), a peak is observed at 4.9 MeV. Around this region the $3/2^+$ and $5/2^+$ states, which have a configuration of $[{}^{12}\text{C}(2^+) \otimes s_{\Lambda}]$, are expected to occur. Millener predicted that the splitting between the states should be 74 keV [27]. The $3/2^+$ and $5/2^+$ states are excited via $\Delta\ell=1$ and $\Delta\ell=3$ transitions, respectively, by the (K^-, π^-) reaction. Accordingly, the yield of γ rays from the $3/2^+$ state to the GS must be much greater than that from the $5/2^+$ state at $0^\circ < \theta_{\pi} < 16^\circ$. The 2^+ peak at around 4.5 MeV is still observed because of insufficient selection of the Λ bound region. A fit to the spectrum was performed using a function consisting of two Gaussians and a linear background in the region from 1.3 to 7.8 MeV. As a result of the fitting, the position of the $3/2^+$ peak was found to be $4.914 \pm 0.010(\text{stat})$ MeV. The width of the $3/2^+$ peak was $220 \pm 25(\text{stat})$ keV (FWHM) which is the same as the width of the 2^+ peak in Fig.6(a). The Doppler shift correction was typically less than 1 % of the γ ray energy, which made the width of the $3/2^+$ peak narrower by 60 keV (FWHM). This result is consistent with identifying that peak as being due to γ rays from ${}_{\Lambda}^{13}\text{C}$ hypernuclei.

After the final energy calibration, the excitation energy of the $3/2^+$ state in ${}_{\Lambda}^{13}\text{C}$ was obtained as $4.880 \pm 0.010(\text{stat}) \pm 0.017(\text{syst})$ MeV. Most of the systematic error originated from the uncertainty of the energy calibration using γ rays from ${}^{12}\text{C}$ nuclei. The present measurement is consistent with the excitation energy of $E_x = 4.89 \pm 0.07$ MeV (preliminary) obtained by the ${}^{13}\text{C}(\pi^+, K^+) {}_{\Lambda}^{13}\text{C}$ experiment [28]. By virtue of the better energy resolution of NaI detectors, a more accurate measurement was achieved.

C. High energy γ rays

γ ray spectra in the high energy region obtained in coincidence with the ${}^{13}\text{C}(K^-, \pi^-)$ reaction at $0^\circ < \theta_{\pi} < 16^\circ$ are shown in Fig.7, where (a) shows γ rays from the quasi-free region and (b) shows those from the Λ bound region. The Doppler shift due to the recoil of a ${}_{\Lambda}^{13}\text{C}$ nucleus was corrected for event-by-event only in Fig.7(b).

In Fig.7(a), a dominant peak at 15 MeV, which corresponds to γ rays from the 1^+ ($T=1$) state to the GS in ${}^{12}\text{C}$, is observed. The 1^+ state in ${}^{12}\text{C}$ is frequently produced by Λ escape from highly excited states in ${}_{\Lambda}^{13}\text{C}$. A fit to the spectrum using the energy resolution assumed by the GEANT simulator resulted in a peak energy of $15.289 \pm 0.022(\text{stat})$ MeV which was shifted to higher energy by 189 keV. The energy shift of the peak was also used for the γ ray energy calibration. The ratio between the yields of γ rays from the 2^+ and 1^+ states in ${}^{12}\text{C}$ is roughly 2:1. This value is not inconsistent with the strength ratio of the states excited

by the $^{13}\text{C}(\text{p}, \text{d})$ reaction [29], which suggests that a quasi-free knockout of a Λ particle is dominant in highly excited regions.

In Fig.7(b), a single peak is clearly observed at 11 MeV, and a small bump, which is due to γ rays from ^{12}C nuclei, is also observed at 15 MeV. γ rays from the $1/2^-$ and $3/2^-$ states in ^{13}C are expected to have almost similar yields by considering theoretical differential cross sections and the acceptance of the spectrometer estimated by the GEANT simulator. However, there is no other prominent peak than that at 11 MeV. It is natural to think that the observed single peak might include γ rays from both the $1/2^-$ and $3/2^-$ states, although this consideration is inconsistent with a previous result that a peak structure, which was considered to be the $3/2^-$ state, was observed at $E_x=9.92\pm0.13(\text{stat})\pm0.5(\text{syst})$ MeV (preliminary) [28]. The energy resolution and strength ratio between the full energy and single escape peaks are estimated to be 0.35 MeV (FWHM) and 2:1, respectively, for 11 MeV γ rays. The width of the observed single peak seems quite consistent with the instrumental peak width, which means that the $1/2^-$ and $3/2^-$ states are close to each other.

D. Splitting of the $1/2^-$ and $3/2^-$ states

As explained in Sec.IIA, the angular distributions of the $^{13}\text{C}(K^-, \pi^-)\Lambda^{13}\text{C}$ reaction selectively excite either the $1/2^-$ or $3/2^-$ states even if the states are not separated in the energy spectrum of γ rays. It is one of the important advantages of our experiment. The events shown in Fig.7(b) were sub-divided into three spectra in Fig.8, where the scattering angles of (a) $0^\circ < \theta_\pi < 7^\circ$, (b) $7^\circ < \theta_\pi < 10^\circ$, and (c) $10^\circ < \theta_\pi < 16^\circ$ were selected. Full energy peaks at 11 MeV are distinctly observed in all spectra.

A response function of the NaI detectors for 11 MeV γ rays was obtained by the GEANT simulator which included the detector geometry and a procedure for adding the energies of the NaI detectors. The response function was folded into the energy resolution of 0.35 MeV (FWHM) which was estimated by assuming a $\sqrt{E_\gamma}$ dependence. Fits to the spectra were performed in the region from 7.5 to 14 MeV using an exponential function for the continuous background and the response function for the peak structures. As a result of the fittings, peak positions of the γ rays were obtained as 11.103 ± 0.029 MeV, 11.016 ± 0.024 MeV, and 10.980 ± 0.032 MeV at $0^\circ < \theta_\pi < 7^\circ$, $7^\circ < \theta_\pi < 10^\circ$, and $10^\circ < \theta_\pi < 16^\circ$, respectively. The errors are statistical only. The fittings gave $\chi^2/\text{N}=1.27$, 0.88, and 0.87, respectively. The surplus at around 10 MeV in Fig.8(a) made the χ^2/N worse. However, the influence of the surplus on the result of the peak position must be little because it is far enough from the peak. The excitation energies and systematic errors of the $1/2^-$ and $3/2^-$ states are derived in Sec.IV.

The splitting of the $1/2^-$ and $3/2^-$ states was extracted from Fig.9, where the peak positions of γ rays are plotted as a function of calculated yield ratio,

$$R = (N(1/2^-) - N(3/2^-))/(N(1/2^-) + N(3/2^-)). \quad (1)$$

$N(1/2^-)$ and $N(3/2^-)$ stand for the yields of γ rays from the $1/2^-$ and $3/2^-$ states, respectively. The yields were calculated using the theoretical differential cross sections of the two states shown in Fig.1 and the acceptance of the spectrometer. The solid angles of the angular regions were 15.0 msr ($0^\circ < \theta_\pi < 7^\circ$), 14.5 msr ($7^\circ < \theta_\pi < 10^\circ$), and 24.1 msr ($10^\circ < \theta_\pi < 16^\circ$).

The right, center, and left closed circles indicate the peak positions measured at $0^\circ < \theta_\pi < 7^\circ$, $7^\circ < \theta_\pi < 10^\circ$, and $10^\circ < \theta_\pi < 16^\circ$, respectively. A fit to the data points was performed with a linear function by considering the statistical errors indicated by bars. As a result of the fitting, a linear function gave $\Delta E(1/2^- - 3/2^-) = +152 \pm 54(\text{stat})$ keV for the splitting of $^{13}\Lambda$ C. This splitting will broaden the peak width of the 11 MeV γ rays by less than 5 %, which justifies the fitting with the response function of a single γ ray for each spectrum in Fig.8.

IV. DISCUSSION

We obtained the splitting of the $1/2^-$ and $3/2^-$ states as $152 \pm 54(\text{stat})$ keV. Different sources of the systematic error for the splitting are discussed below and their contributions are summarized in Table I.

In this analysis, we relied on theoretical differential cross sections. However the γ ray yield at each scattering angle was not completely consistent with the calculation. The γ ray yields in the peak region were 164 ± 18 ($0^\circ < \theta_\pi < 7^\circ$), 166 ± 18 ($7^\circ < \theta_\pi < 10^\circ$), and 142 ± 21 ($10^\circ < \theta_\pi < 16^\circ$). Whereas the theoretically expected yields were 385 ($0^\circ < \theta_\pi < 7^\circ$), 167 ($7^\circ < \theta_\pi < 10^\circ$), and 179 ($10^\circ < \theta_\pi < 16^\circ$). If we assume that these inconsistencies originate from uncertainties in the theoretical differential cross sections, R in Fig.9 would vary as $0.77^{+0.23}_{-0.31}$ ($0^\circ < \theta_\pi < 7^\circ$), $0.01^{+0.01}_{-0.01}$ ($7^\circ < \theta_\pi < 10^\circ$), and $-0.82^{+0.05}_{-0.18}$ ($10^\circ < \theta_\pi < 16^\circ$). The uncertainty of R produced a systematic error of 30 keV as the maximum deviation from the central value for the splitting. This systematic error is the largest one. All possible causes of the inconsistent γ ray yield were investigated. But an inconsistency of about a factor of 2 remained. The theoretical differential cross section of the $1/2^-$ state at the forward angles is especially sensitive to the K^- beam momentum of around 0.9 GeV/c. For example, the differential cross section is expected to decrease by a factor of 3 at 1.0 GeV/c [18]. There is a possibility that a small ambiguity of the K^- beam momentum in previous (K^-, π^-) experiments, on which differential cross sections were adjusted theoretically, might produce such a large inconsistency at the forward angles. If it is a cause of the inconsistency, the systematic error would be much smaller.

Several fittings with different functions, such as 2 Gaussians and a linear background, and widths were applied to study how the choice of functions can influence the splitting, and a systematic error originating from choosing different fitting functions was estimated to be 19 keV at most.

The influence of the Doppler shift correction was also studied by using the GEANT simulator, and it was found to be negligible because the NaI detectors installed symmetrically in the vertical direction almost canceled it. The energy calibration of the NaI detectors affects the splitting very little because γ rays from both the states were measured simultaneously.

The total systematic error of the splitting was estimated to be 36 keV. The final result of the splitting was determined to be $\Delta E(1/2^- - 3/2^-) = +152 \pm 54(\text{stat}) \pm 36(\text{syst})$ keV. The ℓs -splitting of a nucleon in the p -orbit around this mass region is $3 \sim 5$ MeV, thus the ℓs -splitting of a Λ particle in the p -orbit is about $20 \sim 30$ times smaller. After the final energy calibration, the excitation energies of the $1/2^-$ and $3/2^-$ states were obtained as $10.982 \pm 0.031(\text{stat}) \pm 0.056(\text{syst})$ MeV and $10.830 \pm 0.031(\text{stat}) \pm 0.056(\text{syst})$ MeV, respectively. The uncertainty of the energy calibration using γ rays from ^{12}C nuclei and the

choice of fitting functions were mainly considered to estimate the systematic errors. The $j_\Lambda = \ell_\Lambda - 1/2$ ($(p_{1/2})_\Lambda$) state appears higher in energy, as in normal nuclei, which is consistent with theoretical predictions [14,30]. The present measurement is consistent with a γ ray energy of $10.95 \pm 0.1(\text{stat}) \pm 0.2(\text{syst})$ MeV in Ref. [17].

Recently YN interactions were refined in both the OBE model [31] and the quark model [32,33]. The strength of a Λ -nucleus ALS force is different between the models. According to calculations by Hiyama *et al.* in the framework of the microscopic $3\alpha + \Lambda$ model, the ALS force of the OBE models decreased the splitting of $^{13}_\Lambda\text{C}$ by only $20\sim30\%$ [30]. The predicted splittings were 0.75, 0.96, and $0.39\sim0.78$ MeV by means of Nijmegen model D, Nijmegen model F, and Nijmegen soft-core models (a~f), respectively. These calculations systematically show that the YN interaction given by the OBE models predicts larger ℓs -splittings than the present measurement. The state-of-the-art calculation of the YN interaction based on the OBE models is unable to reproduce the present result. On the other hand, in a calculation of the strength of the one-body ℓs -force starting from a quark-based YN interaction, the strength of the ALS force amounted to approximately 85 % of that of the ℓs -force [33]. A calculation using a large ALS force based on the quark model gave about 0.2 MeV for the splitting of $^{13}_\Lambda\text{C}$ [30]. The difference between these results was mainly due to different strengths of the ALS force.

Since the splitting for $^{13}_\Lambda\text{C}$ is very small, forces besides the ℓs -force may also contribute to the splitting. It has been pointed out by Millener that a tensor force makes a significant contribution to the splitting of $^{13}_\Lambda\text{C}$ [34]. The nuclear ℓs -force mixes a small $spin=1$ component into the ^{12}C core wave function, and other forces arise from the $spin=1$ component. His prediction for the splitting of $^{13}_\Lambda\text{C}$ was 107 keV, where the spin-spin force (+42 keV), the ℓs -force (+280 keV), and the tensor force (-215 keV) were considered. The result almost reproduces the present measurement.

A systematic study of light Λ -hypernuclei shows that the YN interactions based on the OBE model need to be modified so that a smaller ℓs -splitting, which has been indicated by the present experiment, can be accommodated [27]. A new mechanism will be required for the unified understanding of the baryon-baryon (NN , YN and YY) interaction.

V. SUMMARY

We performed the $^{13}\text{C}(K^-, \pi^- \gamma)^{13}\text{C}$ experiment at 0.93 GeV/c at the AGS of BNL to obtain the ℓs -splitting of Λ single particle states in $^{13}_\Lambda\text{C}$ with high precision. We succeeded in measuring γ rays from the $1/2^-$ and $3/2^-$ states, which have predominantly a $[^{12}\text{C}_{g.s.}(0^+) \otimes p_\Lambda]$ configuration, to the GS in ^{13}C by using NaI detectors. The splitting was found to be $\Delta E(1/2^- - 3/2^-) = +152 \pm 54(\text{stat}) \pm 36(\text{syst})$ keV which was almost $20\sim30$ times smaller than that of single particle states in nuclei around this mass region. The excitation energies of the $1/2^-$ and $3/2^-$ states were obtained as $10.982 \pm 0.031(\text{stat}) \pm 0.056(\text{syst})$ MeV and $10.830 \pm 0.031(\text{stat}) \pm 0.056(\text{syst})$ MeV, respectively. The $j_\Lambda = \ell_\Lambda - 1/2$ ($(p_{1/2})_\Lambda$) state appeared higher in energy, as in normal nuclei, which is consistent with theoretical predictions. We also observed γ rays from the $3/2^+$ state to the GS in $^{13}_\Lambda\text{C}$, and the excitation energy of the state was obtained as $4.880 \pm 0.010(\text{stat}) \pm 0.017(\text{syst})$ MeV.

ACKNOWLEDGMENTS

We thank the staff of the Brookhaven AGS for their support in running the experiment. We thank Prof. T. Motoba and Prof. K. Itonaga for calculations of angular distributions. We thank Ms. Elinor Norton in the Chemistry Department at BNL for determining the ^{13}C enrichment in our benzene target. We thank Prof. D. Alburger for the careful reading and correcting of the manuscript. We are grateful to Prof. K. Imai for his continuous support to the experiment. This experiment is financially supported in part by the Grant-in-Aid for Scientific Research in Priority Areas (Strangeness Nuclear Physics) 08239205 and for International Scientific Research 10044086 and in part by the U.S. Department of Energy under contract No. DE-AC02-98CH10886.

REFERENCES

- [1] R. E. Chrien and C. B. Dover, *Annu. Rev. Nucl. Science* **39** 113 (1989).
- [2] P. H. Pile *et al.*, *Phys. Rev. Lett.* **66** 2585 (1991).
- [3] T. Hasegawa *et al.*, *Phys. Rev. Lett.* **74** 224 (1995).
T. Hasegawa *et al.*, *Phys. Rev. C* **53** 1210 (1996).
- [4] S. Ajimura *et al.*, *Phys. Rev. Lett.* **86** 4255 (2001).
- [5] W. Brückner *et al.*, *Phys. Lett.* **79B** 157 (1978).
- [6] A. Bouyssy, *Phys. Lett.* **91B** 15 (1980).
- [7] M. May *et al.*, *Phys. Rev. Lett.* **47** 1106 (1981).
- [8] M. May *et al.*, *Phys. Rev. Lett.* **51** 2085 (1983).
- [9] T. Nagae *et al.*, *Int. INS symp. on Nuclear and Particle Physics with meson beams in the 1 GeV/c region*, ed. S. Sugimoto and O. Hashimoto 175 (Universal Academic Press, Tokyo 1995).
- [10] R. H. Dalitz *et al.*, *Nucl. Phys.* **A625** 71 (1997).
- [11] M. M. Nagels *et al.*, *Phys. Rev. D* **12** 744 (1975); **15** 2547 (1977); **20** 1633 (1979).
- [12] C. Dover and A. Gal, in *Progress in Particle and Nuclear Physics*, ed. D. Wilkinson vol.12 171 (Pergamon Oxford 1984).
- [13] Y. Yamamoto and H. Bando, *Prog. Theor. Phys.* **73** 905 (1985).
- [14] K. Itonaga *et al.*, *Prog. of Theor. Phys.* **84** 291 (1990).
- [15] O. Morimatsu *et al.*, *Nucl. Phys.* **A420** 573 (1984).
- [16] H. J. Pirner and B. Povh, *Phys. Lett.* **114B** 308 (1982).
- [17] M. May *et al.*, *Phys. Rev. Lett.* **78** 4343 (1997).
- [18] Private communication with T. Motoba.
- [19] T. Kishimoto *et al.*, AGS research proposal E929 (1996).
- [20] P. H. Pile *et al.*, *Nucl. Inst. and Meth.* **A321** 48 (1992).
- [21] S. Ajimura *et al.*, *Nucl. Inst. and Meth.* **A459** 326 (2001).
- [22] H. Kohri, PhD thesis, Osaka univ., 2000, unpublished.
- [23] R. W. Stotzer *et al.*, *Phys. Rev. Lett.* **78**. 3646 (1997).
- [24] P. Khaustov *et al.*, *Phys. Rev. C* **61** 054603 (2000).
- [25] V. Sum *et al.*, *Nucl. Inst. and Meth.* **A326** 489 (1993).
- [26] K. Hosono *et al.*, *Nucl. Phys.* **A343** 234 (1980).
- [27] Private communication with D. J. Millener.
- [28] O. Hashimoto *et al.*, *Nucl. Phys.* **A639** 93c (1998).
- [29] P. R. Lewis *et al.*, *Nucl. Phys.* **A474** 499 (1987).
- [30] E. Hiyama *et al.*, *Phys. Rev. Lett.* **85** 270 (2000).
- [31] T. A. Rijken *et al.*, *Phys. Rev. C* **59** 21 (1999).
- [32] Y. Fujiwara *et al.*, *Phys. Rev. Lett.* **76** 2242 (1996).
- [33] M. Kohno *et al.*, in *Abstracts of the APCTP Workshop on Strangeness Nuclear Physics*, Seoul, 77 (1999).
- [34] D. J. Millener, *Nucl. Phys.* **A691** 93 (2001).

FIGURES

FIG. 1. Theoretically calculated differential cross sections of the $1/2^-$ (solid curve) and $3/2^-$ (dotted curve) states excited by the $^{13}\text{C}(K^-, \pi^-)\Lambda^{13}\text{C}$ reaction at 0.9 GeV/c.

FIG. 2. The detector system at the target region is shown schematically. See text for a description of each detector element.

FIG. 3. Acceptance of the 48D48 spectrometer obtained for the $^{13}\text{C}(K^-, \pi^-)$ reaction.

FIG. 4. A γ ray energy spectrum of a central NaI detector obtained in an energy calibration run using the $^{58}\text{Ni}(n, \gamma)^{59}\text{Ni}$ reaction. A ^{244}Cm - ^{13}C source was used as a neutron source.

FIG. 5. Momentum vs lab scattering angle spectra (a, c, and e) and excitation energy spectra of ^{13}C at $0^\circ < \theta_\pi < 16^\circ$ (b, d, and f) are shown. Spectra (a-b), (c-d), and (e-f) are before the first stage of event selection (about 10 % of all data), after the first stage, and after the second stage, respectively.

FIG. 6. Energy spectra of low energy γ rays obtained in coincidence with the $^{13}\text{C}(K^-, \pi^-)$ reaction at $0^\circ < \theta_\pi < 16^\circ$. The quasi-free region was selected in (a), and the Λ bound region was selected in (b).

FIG. 7. Energy spectra of high energy γ rays obtained in coincidence with the $^{13}\text{C}(K^-, \pi^-)$ reaction at $0^\circ < \theta_\pi < 16^\circ$. The quasi-free region was selected in (a), and the Λ bound region was selected in (b).

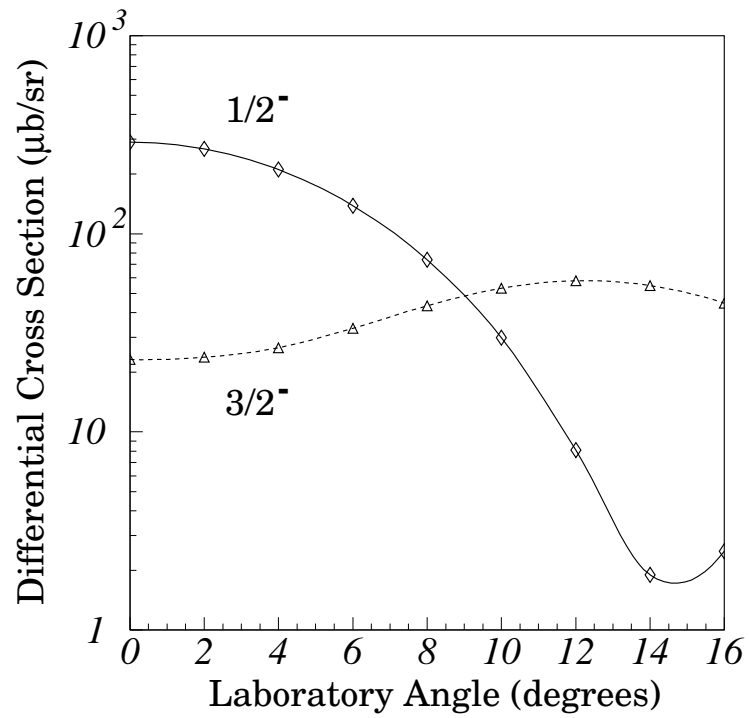
FIG. 8. Energy spectra of γ rays from the Λ bound region obtained in coincidence with the $^{13}\text{C}(K^-, \pi^-)$ reaction at $0^\circ < \theta_\pi < 7^\circ$ (a), $7^\circ < \theta_\pi < 10^\circ$ (b), and $10^\circ < \theta_\pi < 16^\circ$ (c). Dashed and dotted lines show response functions and exponential backgrounds, respectively. Solid lines show the total of them.

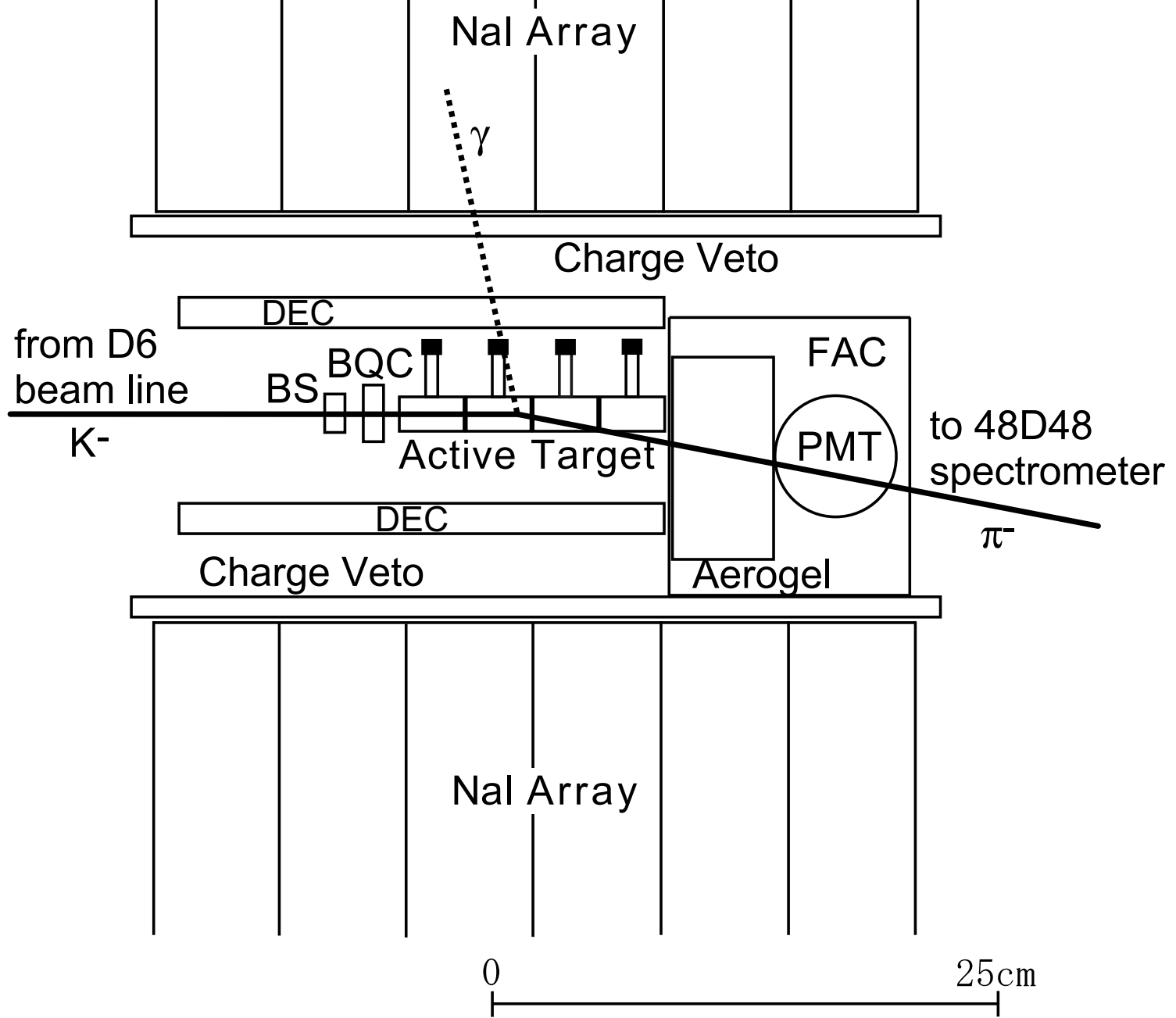
FIG. 9. Peak positions obtained by fitting the γ ray spectra are shown as a function of yield ratio (R). See text for the definition of R.

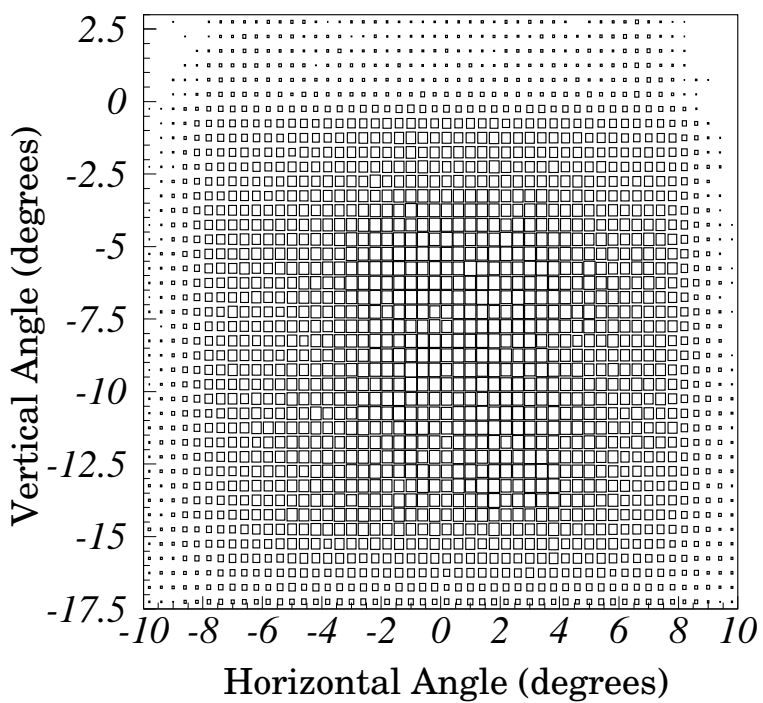
TABLES

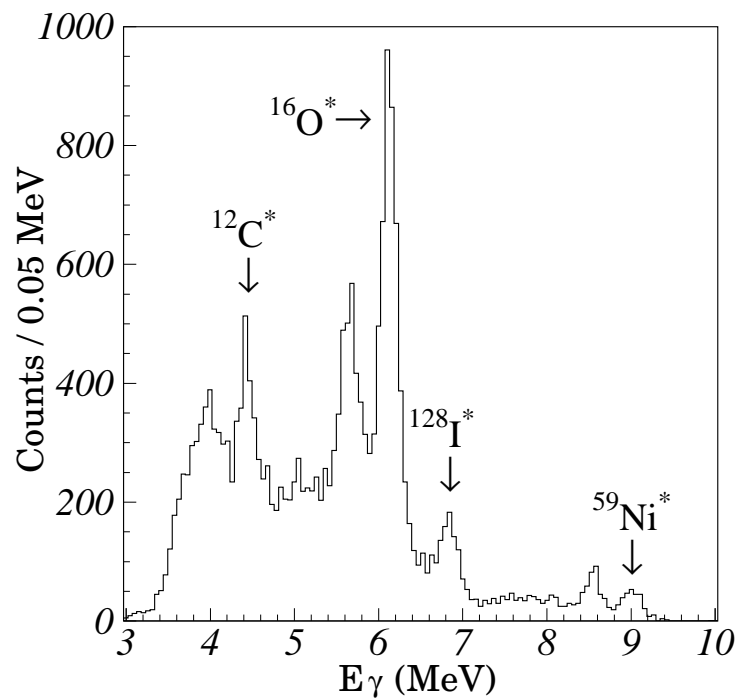
TABLE I. Summary of systematic errors for the splitting.

Effect	Systematic Error (keV)
Cross section uncertainty	30
Fits to spectra	19
Doppler shift correction	1
Energy calibration of NaI detectors	1
Total	36









π momentum (GeV/c)

